7th Asian-Pacific Conference on Aerospace Technology and Science, 7th APCATS 2013

Aerodynamic and Aerothermal Performance of Power-law Shaped Leading Edge of Hypersonic Waveriders

F. M. Wang[a],*, H. Q. Han[a], M. F. Lei[a], J. Zhang[a]

[a]State Key Laboratory of High-temperature Gas Dynamics Institute of Mechanics, Chinese Academy of Sciences
No.15 Beisihuanxi Road, Beijing 100190 P. R. China

Abstract

A numerical study is presented on three- dimensional power-law shaped leading edge for waveriders in hypersonic flow. This work is motivated by interest in researching the flow field properties of power-law shaped leading edge as a possible candidate for blunting leading edges of waveriders. Both aerodynamic and aerothermal characteristics are calculated for a waverider forebody in hypersonic flow. Comparisons are made between power-law shaped leading edges and round leading edge. For the flow conditions considered, the power-law leading edges of waveriders can provide small drag, and at the same time it can bring enough bluntness for the necessity of thermal protection.

Keywords: hypersonic, aerothermal protection, power-law leading edge, aerodynamic performance

---

Nomenclature

a	constant in power-law body equation
H	body height at the base(m)
l	wedge length(m)
n	body power-law exponent
R	circular cylinder radius(m)
x, y	Cartesian axis in physical space
Greek symbols	
θ	wedge half-angle(deg)

---

* Corresponding author.
E-mail address: wangfm@imech.ac.cn

1. Introduction

For hypersonic flying at high attitude, the poor performance that vehicles suffer can be attributed to the strong viscous effect (high skin friction drag) and strong shock wave (high wave drag), which prevent vehicles to achieve the curve called "L/D barrier" given by Kuchemann [1]. The waveriders [2] have shown a great

Promise in breaking the "L/D barrier" and deserve great consideration in the future hypersonic vehicle design. The waveriders usually use reverse design method, it can catch the hypersonic shock at the leading edge which could separates the higher pressure on the lower surface and the lower pressure on the upper surface.

The vehicle leading edges must be sufficiently blunt in order to reduce the heat flux to acceptable level, and possible to allow for internal heat conduction. On the other hand, the reduction in heating flux for a blunt body is accompanied by an increase of wave drag. Therefore, designing a hypersonic vehicle leading edge involves a tradeoff between making the leading edge sharp enough to obtain acceptable aerodynamic efficiency and blunt enough to alleviate aerodynamic heating problem in the leading edge region [3].

The leading edge shape is of considerable practical as well as theoretical interest to both the aerodynamic force and aerodynamic heating. Usually, a round leading edge with constant radius has been chosen for blunting geometry. Nevertheless, shock detachment distance on a round leading edge, as well as associated leakage, scales with the radius of blunted leading edge. Power-law shapes ($y \propto x^n$, $0 < n < 1$) may provide the required bluntness for aerodynamic and aerothermal concerns, which is based on Mason and Lee's work [4]. Santos has done some researches on the aerodynamic performance of two-dimensional power-law leading edges using Direct Simulation Monte Carlo (DSMC) method [5, 6]. However, stagnation point heat flux and heat load of leading edge, as important aspects for this problem, were not considered.

The focus of the present study is to find a way to modify the leading edge of waveriders which could obtain aerodynamic benefit and satisfy the necessity of thermal protection. Power-law shaped leading edges, as possible candidate for blunting geometries of hypersonic leading edges, will be compared to round leading edges in order to determine which geometry would be better as a blunting profile in terms of total drag and stagnation point heating. The physical model is a waverider produced for freestream Mach number of 6 and attitude of 30km. The investigations of aerodynamic and aerothermal properties will be conducted for power-law shaped leading edge waveriders with various power-law exponents and compared with generally round one.

2. Leading edge geometry definition

In two-dimensional form, the power-law shapes are given by the following expression:

$$y = ax^n \tag{1}$$

Where n is the power-law exponent ($0 < n < 1$) and a is a constant which is a function of n. The power-law shapes given by Eq. (1) have radius of curvature $R(x)$ of

$$R(x) = \frac{1}{|n(n-1)a|} \left[x^{2/3(2-n)} + (na)^2 x^{(4/3n-2/3)} \right]^{3/2} \tag{2}$$

Taking the limit of Eq. (2) as $x \to 0$, we got three distinct classes of results for the radius of curvature, depending on the value of n:

n	$R(0)$
>1/2	0
=1/2	$a^2/2$
<1/2	∞

For those power-low leading edges, when $n>1/2$, the leading edge radius of curvature is zero, which are geometrically blunt. On the contrary, When $n<1/2$, the leading edges are geometrically blunt. Only one value of n produces a nonzero finite value for the leading edge radius of curvature.

The present power-law shape is modeled by assuming a sharp leading edge of half angle θ with a circular arc of radius R inscribed tangent to this wedge. Fig. 1 illustrates the construction for power-law shaped leading edge, where l is the wedge length and the common body height H is the distance from tangent point to x axis.
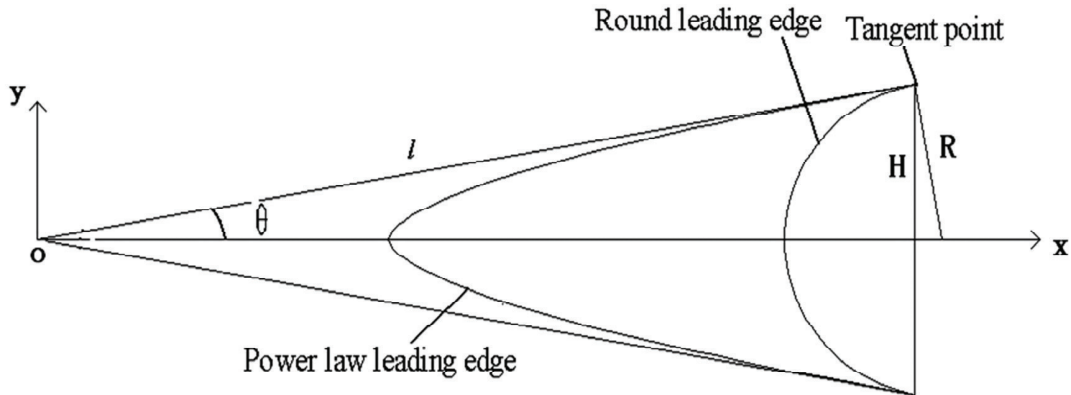

Fig. 1 Leading edge geometry

The x-coordinate of tangent point is given as unity. The radius R of tangent circular arc, wedge length l and body height H are satisfied with the following relations:

$$\begin{cases} H = \tan(\theta) \\ R = \dfrac{\sin(\theta)}{\cos^2(\theta)} \\ l = \dfrac{R}{\tan(\theta)} \end{cases} \tag{3}$$

Now the power-law shaped leading edge in the coordinate shown in Fig. 1 is expressed as following:

$$y = a(x - b)^n \tag{4}$$

In order to illustrate the exponent efficiency in power-law shaped leading edge, for example, it is assumed a wedge half angle of 10 deg, and power-law exponents of 0.2, 0.4, 0.6 and 0.8. Fig. 2 shows that the leading edge shaped by power-law exponent of 0.8 is very sharper, and the leading edge shaped by the exponent of 0.2 is blunter than circular arc. We chose three different power-law shaped leading edges with exponents of 0.4, 0.5 and 0.6, which are geometrically blunt, finite radius of curvature and geometrically sharp, respectively.
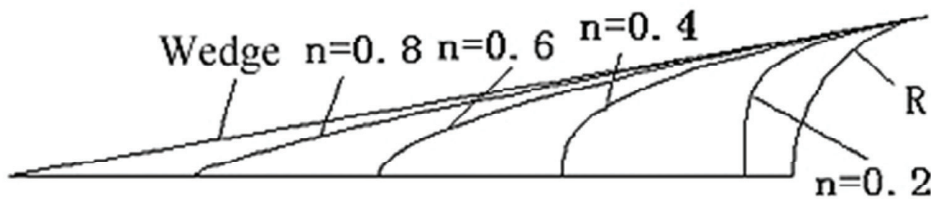

Fig. 2 Sketch of power-law leading edge with various power-law exponents

Round leading edge   n=0.4
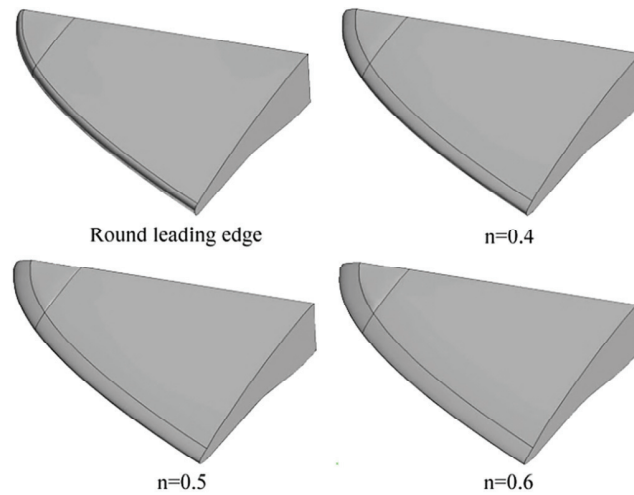
n=0.5   n=0.6

Fig. 3 Waveriders forebody with round and power-law leading edge

In order to analyze and validate the availability of power-law shaped leading edges in hypersonic waveriders, a waverider forebody being part of a waverider which is produced at Mach number of 6 and attitude of 30km with maximum L/D is chosen as physical model. Fig. 3 shows the waverider forebodies with round leading edge and power-law shaped leading edges at various power-law exponents, where the half angle is 10 deg.

3. Numerical method

3.1 Summarization of numerical method

A computational fluid dynamics code is used to simulate the aerodynamic and aerothermal performance of the physical models given above. The RANS equations is solved with a route in which, inviscid flux is calculated using AUSM+ scheme, and viscous flux is calculated using second order central scheme, solution reconstruction uses third order MUSCL, and LU-SGS method is used for time discretization. A two-equation Menter's SST $k-\omega$ model is used to close the RANS equations. Details on numerical method refer to Yan Chao' book [7].

3.2 Validation

For validating the effectiveness of present method, the Ames All-Body model [8] shown in Fig. 4 are studied. The forebody is an elliptic cone with a major-to-minor axis ratio of 4, and the afterbody has elliptic cross sections with a sharp straightline trailing edge. The juncture between the forebody and the afterbody occurs at 2/3 of the body length. The model has a delta planform with leading-edge sweepback of $75°$ and total axial length L of 0.9144m. The case was for a freestream Mach number of 7.4 and Reynolds number based on the body length of $15×10^6$. The freestream static temperature T_∞ and the model wall temperature T_w were 62K and 300K respectively.
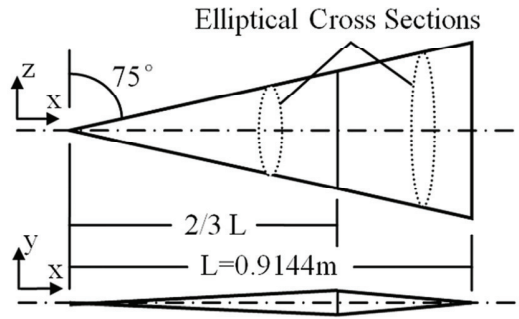
Fig. 4 Schematic of Ames All-Body model

Fig. 5 shows the variation of the centerline pressure distribution with angle of attack. The centerline pressure ratio (ratio of centerline pressure to freestream static pressure p∞) is plotted versus the axial location x/L along the surface centerline. The present code results compares very well to the experimental data [9]. In addition the surface heat transfer distributions along the centerline are given in Fig. 6 over the same angle of attack range. The Stanton number St $\left\{\text{St} = q / \left[\rho_\infty u_\infty (H_t - H_w) \right] \right\}$ used for the comparisons is based on the surface heat transfer rate q, freestream unit mass flow $\rho_\infty u_\infty$, freestream total enthalpy H_t, and wall enthalpy H_w. For this Fig., the Stanton number is plotted on log-log plots versus the axial location x/L along the surface centerline. There is good agreement between the experimental results and the present code results.
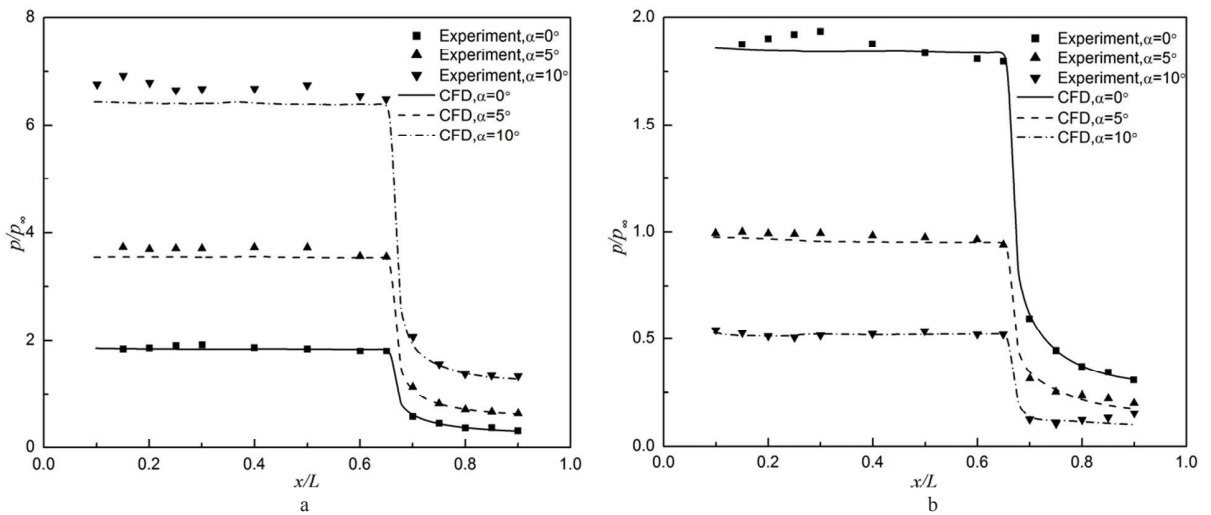

Fig. 5 Ames All-Body model centerline pressure distribution. a Windward; b Leeward
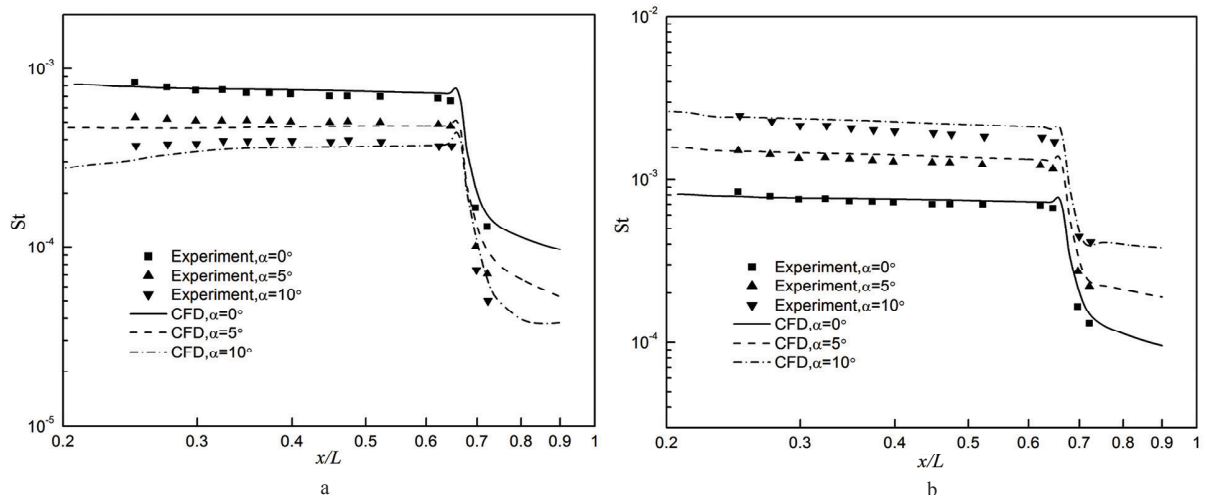
Fig. 6 Ames All-Body model centerline heat transfer distribution. a Windward; b Leeward
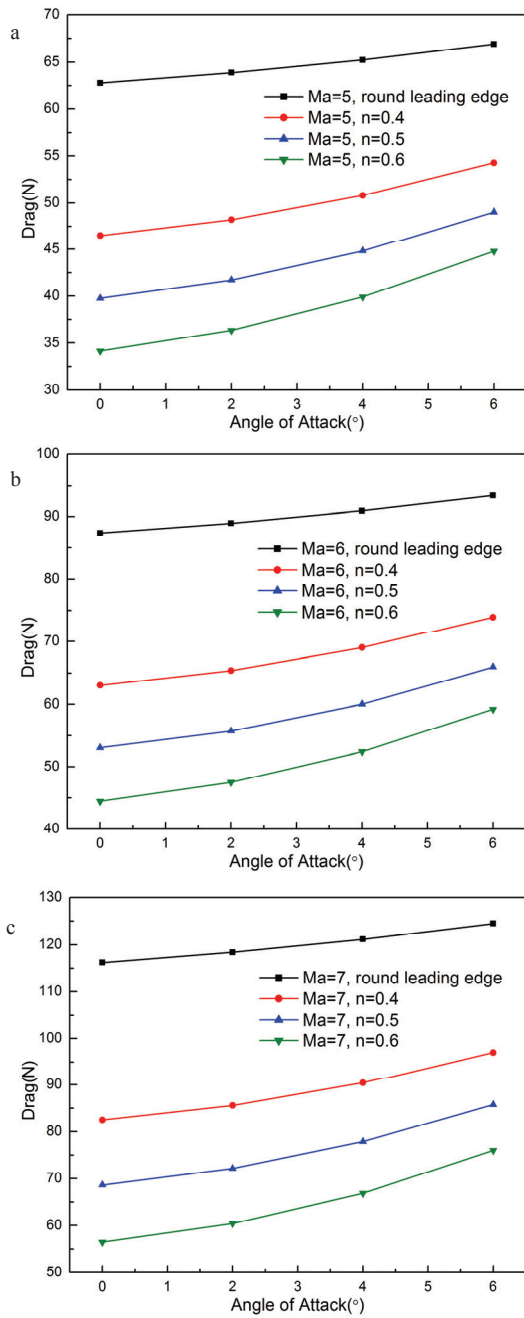
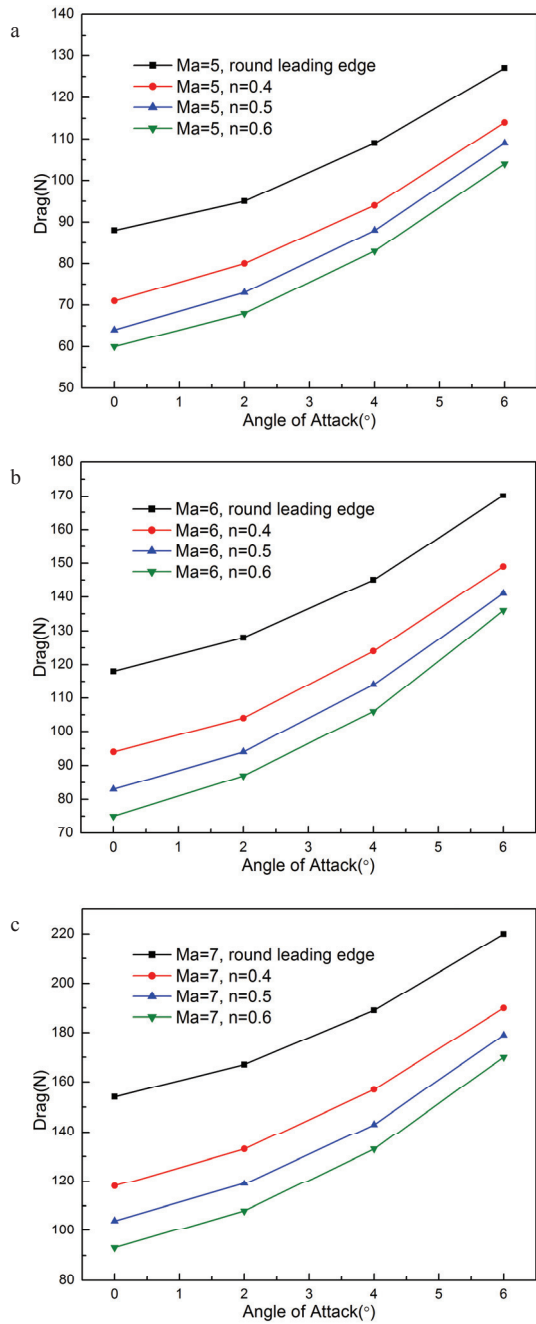Fig. 7 Leading edge drag for different Mach numbers.

a Ma=5; b Ma=6; c Ma=7

Fig. 8 Total drag for different Mach numbers.

a Ma=5; b Ma=6; c Ma=7

4. Computational results and discussion

The computational conditions for this study include nominal freestream Mach number of 5, 6 and 7; 30km atmosphere parameters[10] for freestream; and model angles of attack α of 0, 2, 4 and 6 deg. The constant temperature of 1100K is taken as a wall boundary condition.

Aerodynamic surface, especially the leading edge region, quantities include pressure, heat flux and aerodynamic drag. The purpose of this section is to discuss and to compare the differences of these quantities resulting from various leading edge shapes for waverider forebody.

The aerodynamic drag is obtained by the integration of the pressure and shear stress distributions on a surface, so it can be divided into pressure drag and skin-friction drag. It is important to mention that the values for the drag presented in this section were obtained by assuming that no base pressure effects were taken into account in the calculations. The aerodynamic drag increases with angle of attack increasing as shown in Fig. 7. The drag of power-law shaped leading edge, as compared to round leading edge, decreases obviously. As the power-law exponent n increases, the drag decreases smoothly and the decrease has no rapid change. For the cases we investigated, the major contribution to the aerodynamic drag is attributed to the pressure drag. When the exponent n increases, the leading edge becomes geometrically sharp, which cause the decreasing of pressure drag. Similar tendency can be observed for different Mach numbers.

Now, let us discuss the drag on the whole surface of the waverider forebody with different power-law exponents. Fig. 8 describes the total drag against angle of attack at different power-law exponents. When angle of attack increases, the total drag grows rapidly because the increasing pressure drag of upper face and lower face dominates the total drag. Note that he total drag decreases obviously as the power-law exponent growing. In particular, the total drag of power-law shaped leading edge with exponent of 0.6 decreases by about 30% comparing with the round leading edge at zero angle of attack with freestream Mach number of 5. It is just because that the power-law shaped leading edges behave aerodynamically sharper than round leading edges, which makes shock wave become weaker. At the same time, the shock standoff distance of power-law shaped leading edge is smaller comparing with the round leading edge, which is illustrated in Fig. 9. Therefore, it prevents spillage of the high-pressure airflow from the lower side of the waverider forebody to the upside so as to acquire better aerodynamic performance. It should be emphasized that shock standoff distance is very important to hypersonic vehicles such as waveriders.
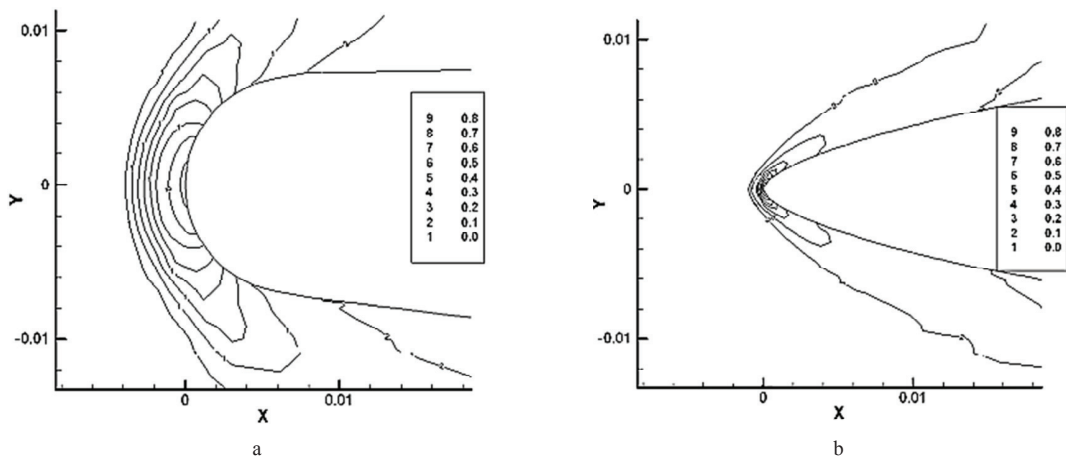

Fig. 9 The contour lines of non-dimensional pressure for different leading edge, Ma=6, α=0° . a Round leading edge b Power-law leading edge, n=0.6
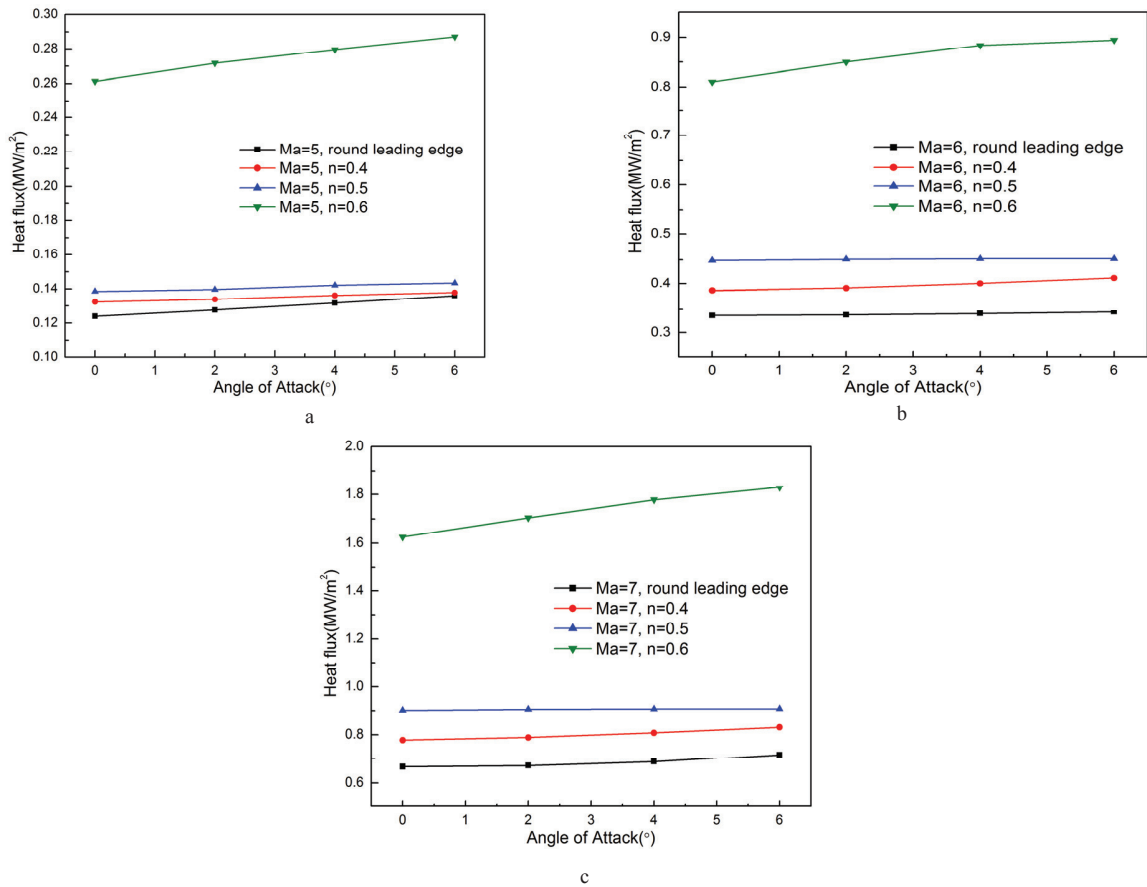
Fig. 10 Leading edge peak heat flux for different Mach numbers. a Ma=5; b Ma=6; c Ma=7

As one important problem of hypersonic vehicles, heat flux peak value cannot be ignored. It indicates concentrated heat flux in local region, which can be used to check the local aerothermal protection stress. The leading edge geometry effect on the heat flux peak value is illustrated in Fig. 10 for power law exponents of 0.4, 0.5 and 0.6. The heat flux peak value shows only a smaller difference with angle of attack increasing from 0º to 6º, but it grows very fast with the freestream Mach number increasing. The curves in Fig. 10 also indicate that the heat flux peak value becomes higher as power-law exponent increases, for power-law shaped leading edge gets sharper with power-law exponent increasing as shown in Fig. 2. Compared with round leading edge, the heat flux for leading edge shaped by power-law exponent of 0.4 or 0.5 increases only a little, but when power-law exponent is 0.6, the heat flux peak value increases rapidly which is nearly twice as large as the heat flux peak value for power-law exponent of 0.4. The reason of this is that geometrically sharp leading edge will produce a high local heat flux. Thus, heat flux peak value for power-law exponents $n>1/2$ is much larger than that of round leading and leading edges with power-law exponents $n<1/2$.

Leading edge heat load is used to describe the whole heat capacity which must be treated by thermal protection system. It is very important for heat pipe design if the cold pipe thermal protection is used. Fig. 11 shows that the leading edge heat load on the leading edge surface shaped by power-law method is bigger than that of round leading edge. Also, it is seen that the heat load is very sensitive to the power-law exponent in the leading edge region. The bigger the power-law exponent is, the higher the leading edge heat load. Moreover, the heat load of

leading edge shaped with power-law exponent of 0.4 or 0.5 is higher than that of the round leading edge about 30%. If the leading edge shaped by the power-law exponent 0.6, it becomes about two times as heat load of round leading edge. Similar with heat flux peak value, leading edge heat load with power-law exponent of 0.6 is much larger than that of the other three cases.
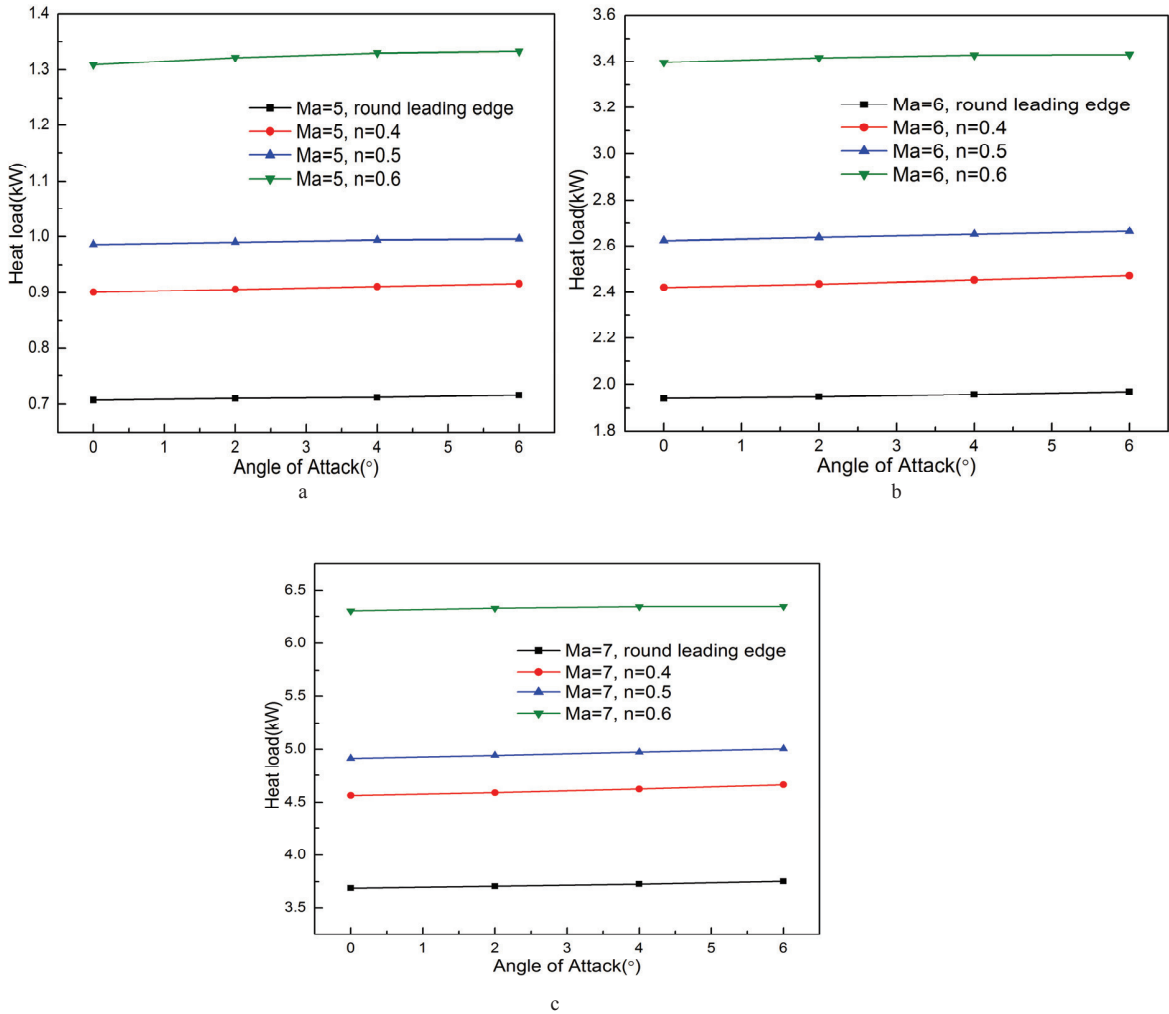

Fig. 11 Leading edge heat load for different Mach numbers. a Ma=5; b Ma=6; c Ma=7

5. Conclusion

The computation of hypersonic flow on a three- dimensional waverider forebody whose leading edge is shaped by power-law method has been conducted. The calculation provided information concerning the nature of aerodynamic quantities on the body surfaces resulting from leading edges shaped by variable power-law exponents. Power-law leading edges were utilized for blunting of waveriders, and aerodynamic and aerothermal properties of power-law leading edges were compared with round leading edge in order to determine which

geometry is better suited as a blunting profile for leading edges of hypersonic vehicles. Power-law shaped leading edges of waveriders are shown to decrease total surface drag and also are blunt enough to reduce aerodynamic heating flux at leading edge region with appropriate selection of power-law exponent. Usually, the power-law exponent can be chosen as $0<n\leqslant1/2$ to avoid excessive heat flux peak value of geometrically sharp leading edges for the power-law exponents $1/2<n<1$. Hence, if both aerodynamic heating and drag are considered for the design of leading edges of hypersonic vehicles, then power-law shaped leading edge will be a useful candidate.

Acknowledgements

References

[1] Kuchemann, D., 1978. The Aerodynamic Design of Aircraft. Pergamon Press, New York.
[2] Nonweiler, T., 1959. Aerodynamic Problems of Manned Space Vehicles. Journal of the Royal Aeronautical Society 63, pp. 521-528.
[3] Bertin, J., Cummings, R., 2006. Critical Hypersonic Aerothermodynamic Phenomena. Annual Review of Fluid Mechanics 38, pp. 129-157.
[4] Mason, W., Lee, J., 1994. Aerodynamically Blunt and Sharp Bodies. Journal of Spacecraft and Rockets 31(3), pp. 378-382.
[5] Santos, W., Lewis, M., 2002. Power-law Shaped Leading Edges in Rarefied Hypersonic Flow. Journal of Spacecraft and Rockets 39(6), pp. 917-925.
[6] Santos, W., 2008. Physical and Computational Aspects of Shock Waves over Power-law Leading Edges. Physics of Fluids 20, 016101.
[7] Yan, C., 2006. Method and Application of Computational Fluid Dynamics (in Chinese). Beihang University Press, Beijing.
[8] Williams, L., 1971. Estimated Aerodynamics of All-Body Hypersonic Aircraft Configurations. NASA Technical Memorandum X-2091.
[9] Lockman, W., Lawrence, S., 1992. Flow over an All-Body Hypersonic Aircraft: Experiment and Computation. Journal of Spacecraft and Rockets 29(1), pp. 7-15.
[10] U.S. Standard Atmosphere. Washington, D.C.: U.S. Government Printing Office, 1976.